# CHAPTER 4

# EXPERIMENTAL SETUP AND PROCEDURE

## 4.1 Description of Experimental Setup

Present investigation used an experimental setup for visualizing multi-phase flows in a vertical annulus charged with water, $Al_2O_3$/water, $TiO_2$/water and $SiO_2$/water nanofluids with a concentration of 0.001%, 0.005% and 0.01% v/v to study the heat transfer characteristics and flow pattern evolution during upward flow boiling in a vertical test section. The effect of supplied heat flux, mass flux, inlet subcooling and particle volume fraction on heat transfer characteristics, bubble behavior and flow regimes have been investigated**.**

The schematic of the experimental setup for subcooled flow boiling heat transfer of nanofluids has been shown in Fig. 4.1. The experimental facility was designed to investigate thermal-hydraulic phenomena associated with flow boiling of water and nanofluids. The actual setup during the experimentation has been shown in Fig. 4.2. The test section was a quartz vertical tube with 1000 mm length, 50 mm outside diameter and 2.5 mm wall thickness. The cylindrical quartz tube concentrically surrounds a stainless steel (SS316 L) cartridge heater of 12 mm dia, with thermocouples brazed on the surface for temperature measurement. The heated length of cartridge heater was 700 mm with unheated length of 50 mm at top and 150 mm at bottom to reduce the hydrodynamic entrance effects. The experimental facility includes the test section assembly, centrifugal pump, data acquisition system, thermocouples, variac, condenser and a preheater. The cartridge heater, with a maximum power of 10 kW was heated by external power source controlled through a variac. The working fluid was supplied through a centrifugal pump

from a reservoir, which was connected to a preheater to obtain the desired degree of subcooling at the inlet. Quartz tube was fabricated with holes at five equidistant locations (175 mm axial interval) through which K-type thermocouples (Omega) were inserted to measure the local heater surface temperature and the liquid bulk temperature. The thermocouples for surface temperature measurement were brazed to the heater surface for accuracy. Two K-type thermocouples were inserted into the flow to measure the fluid bulk temperatures at the inlet and exit of the test section, respectively. The K-type thermocouple was used as it provides more accurate reading for high temperature measurements. The outer diameter of the K-type thermocouple used is 3 mm and its time constant provided by the manufacturer (OMEGA Inc.) is about 0.60 s in water. The thermocouples measured the temperatures during the flow boiling experiments and data acquisition system (National Instruments PXIe 1071) recorded the signals from the thermocouples using Lab view software. Various valves were included in the test loop for loading, flow control and discharge of the working fluid. Present work employed two types of camera, first one (Nikon D5200 single lens reflex camera) to capture the flow patterns and second one (Motion BLITZ Cube High Speed Camera, manufactured by Mikrotron GmbH) to capture the bubble behavior of water and nanofluids. The high-speed video camera was adjusted to focus on nucleating bubbles. In order to capture the very short bubble growth phenomenon, the frame rate was set at1000 frames/s with a resolution of 1280× 1024 pixels. The bubble images obtained by the high speed camera were downloaded to the computer and analyzed using image processing software Image J to measure the bubble diameter for the present experiments.

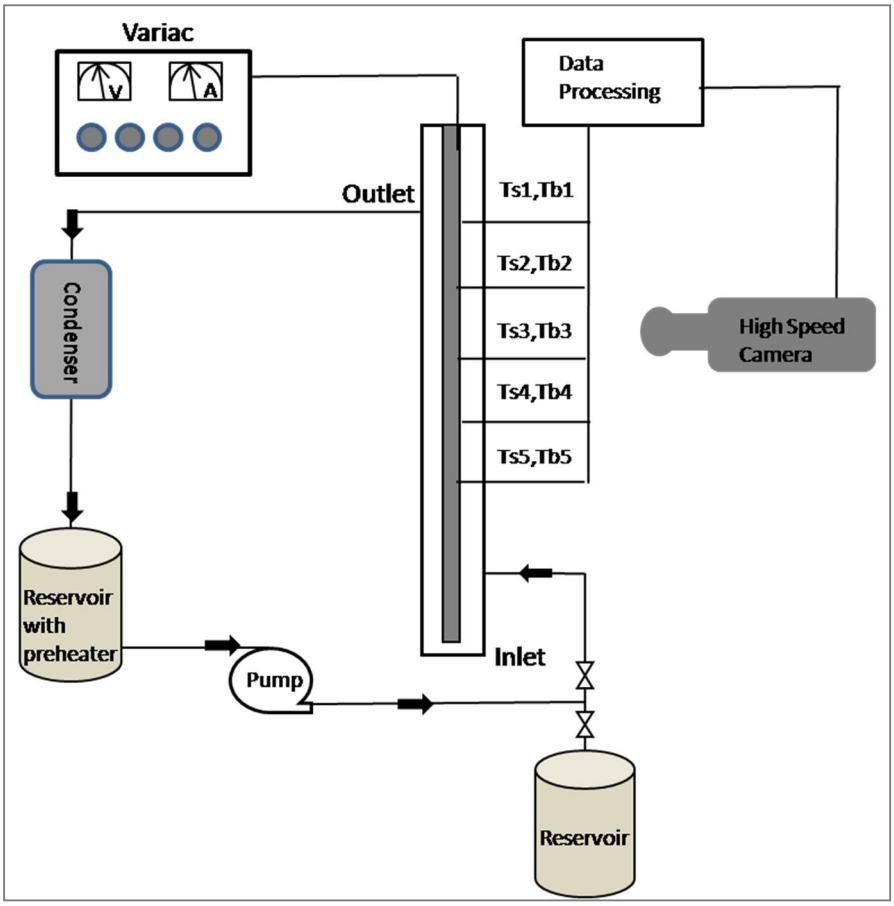


**Fig. 4.1** Schematic of Flow Loop

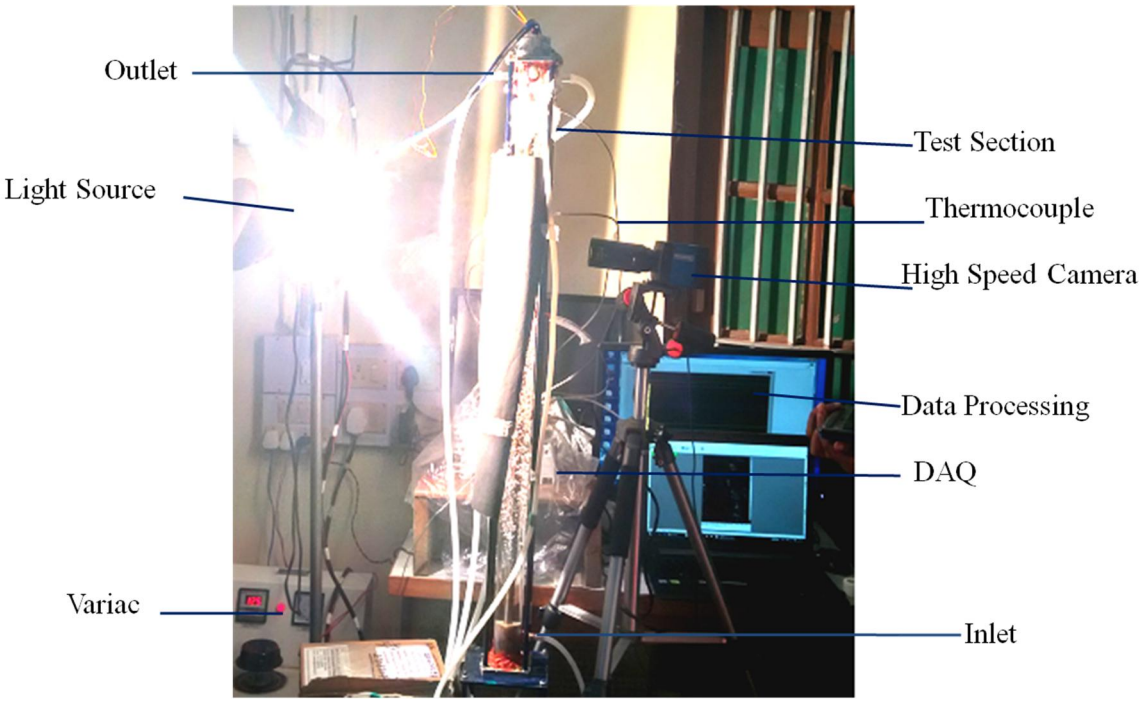


**Fig. 4.2** Test Rig during experimentation

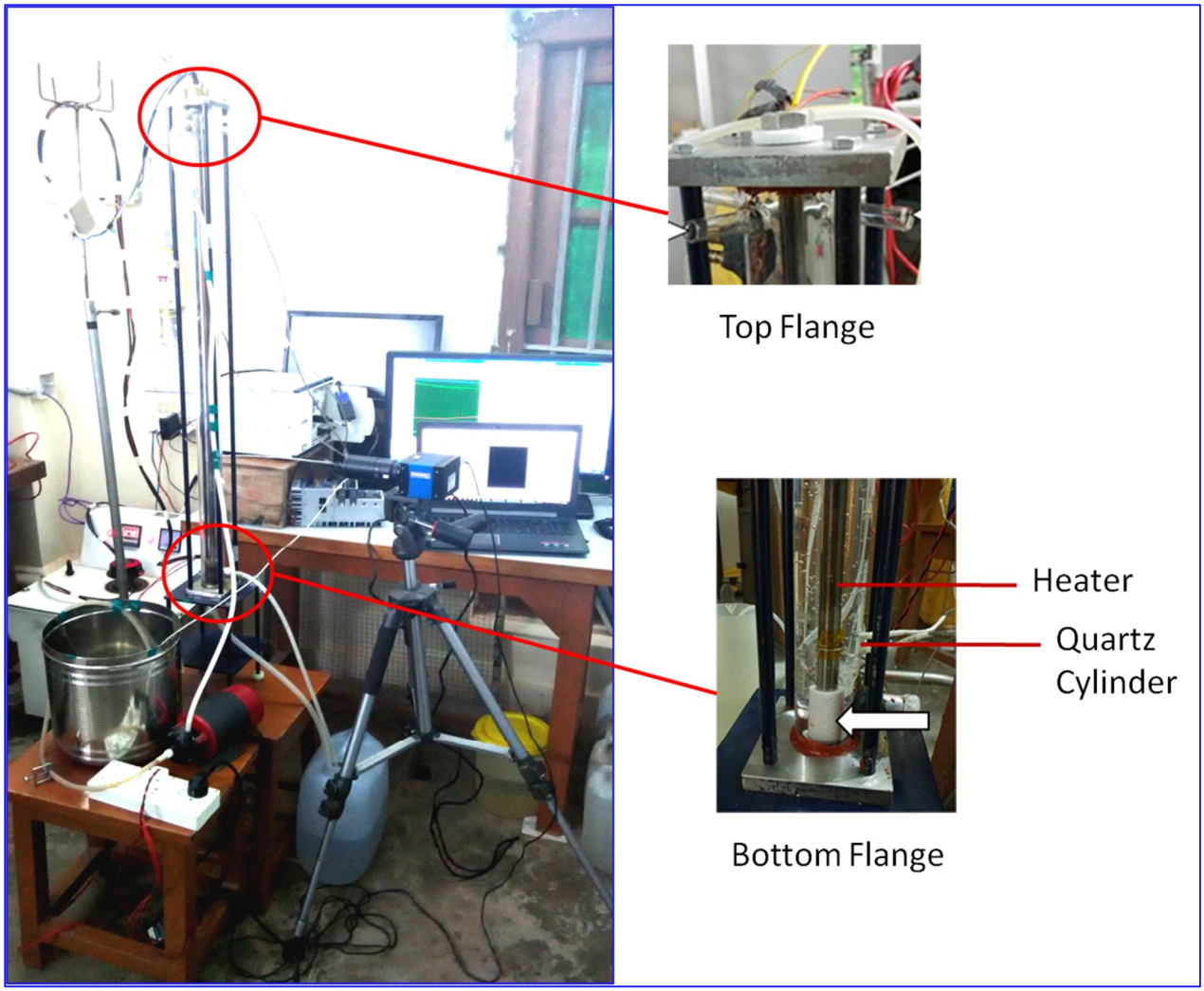


**Fig. 4.3** Test Rig

## 4.2 Instrumentation and Equipment

### 4.2.1 Cartridge Heater

The stainless-steel (SS316 L) tube cartridge heater of 12mm outer diameter is heated by an electric coil with an inbuilt thermocouple to regulate the heater temperature. The heater surface has a length of 1000 mm with unheated portion of 150 mm and 50 mm at the bottom and the top respectively. The heater has 10 kW rated power capacity. Provisions have been made for the thermal expansion and contraction during operation. The lower end of the heater is guided through a Teflon gasket (which can withstand high temperature, shown with white arrow in Fig. 4.3.) at the center of the quartz cylinder

which is fixed to the stainless-steel flange (Bottom flange). This is expected to minimize any buckling of the heater tube due to uneven thermal expansion during the experiment. Red RTV and araldite have been used to make the assembly leak proof. The heater has been provided with a threaded head at the top so that it can be precisely fitted in the top flange. The specifications of the cartridge heater has been provided in Table 4.1.

**Table 4.1** Specifications of the cartridge heater

| Parameters | |
|---|---|
| Sheath Material | SS 316 L Cylindrical Rod |
| Watt Density | 295 W/m$^2$ |
| Watt Rating | 10 kW |
| Voltage | Up to 220V |
| Length | 1000 mm |
| Diameter | 12 mm |
| Controls | Thermocouple |

### 4.2.2 Temperature Measurement

K-type thermocouples have been used for the temperature measurement because of its dependability and precision. It can be used to measure temperature up to 1260 $^oC$. Figure 4.4 shows the K-type thermocouple employed in the research. It contains two wires of 0.5mm diameter that are insulated by fiberglass and sheathed with SS316L. The outer diameter of the thermocouple is 3mm.

**Fig. 4.4** K-type thermocouple

Twelve number of K-type thermocouples have been used in the present work, out of which five were used to measure surface temperature and five for bulk fluid temperature and the rest two were measuring inlet and outlet temperature. Table 4.2 shows the specifications of the thermocouples.

**Table 4.2** Specification of thermocouple

| **Parameters** | |
|---|---|
| Thermocouple Model | K-type |
| Diameter of wires | 0.5 mm |
| Sheath diameter | 3 mm |
| Temperature range | 0 to 1260 $^{o}$C |
| Accuracy | $\pm$ 2.2 $^{o}$C |
| Sheath material | Stainless steel |
| Voltage range | 0 to 10V (DC) |

### 4.2.3 Data Acquisition System (DAQ)

The thermocouples were connected to a National Instruments Data Acquisition System as shown in Fig. 4.5. It is a NI cDAQ-91321.33 GHz Dual-Core Atom, 4-Slot, Compact DAQ Controller. The cDAQ controller features a number of standard interfaces and combines with C Series modules to measure a broad range of analog and digital I/O signals that can be logged to the local hard drive or an SD card.


**Fig. 4.5** NI cDAQ-9132

The software interface used in the DAQ is LabVIEW (Fig. 4.6) which is a graphical programming environment that enables us to measure and control data easily. Temperature data are logged in a TDMS file which can be opened in a spreadsheet.

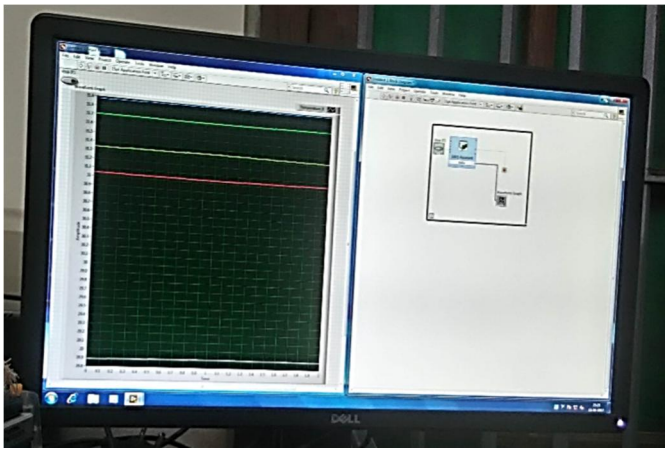

**Fig. 4.6** Labview

### 4.3 Experimental Procedure

The experiments on flow boiling were carried out at atmospheric pressure. The temperature of the working fluid in the reservoir was raised to the desired temperature. The liquid was circulated by a constant speed centrifugal pump and the flow rate was adjusted using the control valves through the test loop. Prior to the experiment, the test loop was heated, and a vigorous forced convective boiling was carried out for approximately 2 hours to expel any trapped gases in the liquid as well as on the heater surface before conducting the experiments. Afterwards, the preheater was activated to reach the target temp at the inlet of the vertical channel. At that time, the power was supplied at a lower input level and allowed to attain steady state. Then small increments were given in power supply until occasional dry patches appeared due to flow oscillation at higher heat flux. At this point the power supply was cut-off. The test section was cleaned with water and acetone after each experimental run with nanofluids to remove the deposition of nanoparticles. The experimental parameters have been listed in Table 4.3.

**Table 4.3** Parameters of the test section and system

| Parameter | Value |
|---|---|
| **Test section characteristics** | |
| Length (mm) | 1000 |
| Outer dia. (mm) | 50 |
| Inner dia. (mm) | 45 |
| **Heater characteristics** | |
| Dia. (mm) | 12 |
| Length (mm) | 980 |
| **Operating Parameters** | |
| Mass flux ($kg/m^2s$) | 3-20 |
| Heat flux ($kW/m^2$) | 30-250 |
| Degree of subcooling (K) | 20, 40, 60 |
| Particle concentration (vol. %) | 0.001, 0.005, 0.01 |

### 4.4 Image Processing

Obtaining images of flow boiling regimes was difficult and complicated by the presence of a large number of small bubbles. Transparent quartz cylinder was fabricated for the test section to provide a view of the heating surface. High magnification with a well-adjusted focus and intense lighting were essential to capture and freeze the flow patterns and the coalescence of bubbles during flow boiling experiments. The transparent quartz cylinder provided optical accessibility enabling images to be taken from the camera on front side using reflected light from the illuminator on the back side. The flow visualization was recorded using a Mikrotron Motion BLITZ Cube 4 high-speed camera at a speed of 1,000 fps (time resolution of 1 ms) and resolution of 1280 × 1024 pixels. As boiling is a periodical process of generation and departure of a bubble or a large vapor clot, a high-speed camera has a fast frame rate synchronized with very short exposure time in order to observe an overall process.

The camera was mounted on a tripod and was aimed at the heater from the side. In order to achieve the highest possible resolution and eliminate errors in calibration, the camera lens was fixed at a constant focal length, resulting in a fixed viewing area. Since the camera was maintained normal to the direction of the flow, the error in measuring the bubble diameter due to optical distortion is minimized.

With the MotionBLITZ – the Digital Motion Analyzer Recorder – rapidly moving or explosive processes can be continuously recorded and stored at up to93,000 images per second and can be displayed and analyzed in detail immediately after the end of a sequence. The images are always initially stored in the internal frame memory of the camera. Because of the built-in rechargeable battery, the camera can operate up to 30 minutes in record mode and can store the recorded data in the internal frame memory for up to 2 hours (and more than 20 hours in case of the standby option). The MotionBLITZ must be connected to a host PC via fast Ethernet only when downloading recorded sequences or when camera parameters need to be modified or changed.

High-speed visualization of the bubble dynamics enabled to observe the bubble growth and flow pattern evolution under various conditions. At a given heat flux, bubble behavior was photographed using the high speed camera (Fig.4.7). Recordings for each experimental conditions were made 2–3 times to ensure the repeatability of the results. The original grayscale images (Fig.4.8) were processed through ImageJ software by means of different techniques and measurements of bubble parameters were carried out. The known diameter of the heater rod (12 mm) was considered as reference for calibration of the length scale. Images were extracted from the video and were analyzed to understand bubble dynamics in water and nanofluids.

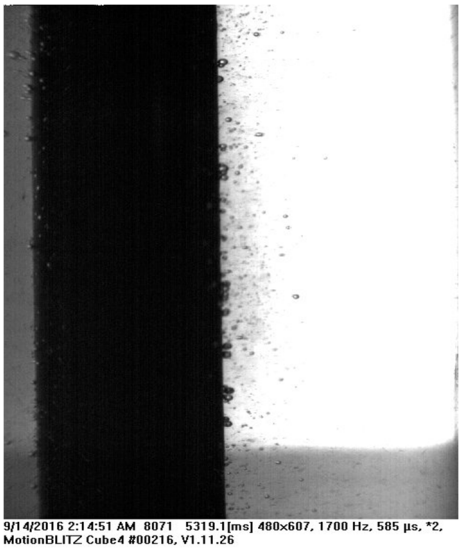


**Fig. 4.7** High Speed Camera **Fig. 4.8** Image obtained after Post Processing

### 4.5 Data Analysis

Heat transfer coefficient is the proportionality constant between the heat flux and the thermodynamic driving force for the flow of heat and shows how effectively heat can be transferred within a system assuming heat loss to surrounding is negligible. Experimental data have been used to calculate the heat transfer coefficient for water and nanofluids.

The heat flux in the test section has been calculated as:

$$q'' = \frac{VI}{\pi DL} \qquad (4.1)$$

Where V is the voltage, I is the current, D and L are the diameter and length of the heater rod.

The heat transfer coefficient has been estimated as:

$$h = \frac{q''}{\Delta T} \qquad (4.2)$$

Where$\Delta T$ = $T_w$-$T_b$, $T_w$ and $T_b$ are surface temperature of the heater and bulk temperature of the fluid respectively.

A common dimensionless value used in heat transfer calculations is called the Nusselt number *Nu,* named after Wilhelm Nusselt. The Nusselt number is the ratio of convective to conductive heat transfer across the boundary of heat transfer, which is defined as:

$$Nu = \frac{hD_h}{k} \tag{4.3}$$

Where, $h$ is the heat transfer coefficient, $D_h$ is the hydraulic diameter of the test section, and $k$ is thermal conductivity of the working fluid.

Another dimensionless value commonly used in heat transfer calculations is the Reynolds number *Re*, named after Osborne Reynolds. The Reynolds number is the ratio of momentum forces to viscous forces which is defined as:

$$Re = \frac{\rho v D_h}{\mu} \tag{4.4}$$

Where, $\rho$ is the density of the test fluid, $v$ is the mean velocity of the working fluid, $D_h$ is the diameter of the test tube, and $\mu$ is the dynamic viscosity of the fluid.

### 4.6 Uncertainty Analysis

An uncertainty analysis was conducted to estimate the uncertainties associated with various parameters using the method proposed by Holman [139]. The method is based on careful specifications of the uncertainties in the various primary experimental measurements. Temperature measurement uncertainties were primarily estimated considering the thermocouple calibration and temperature correction from the thermocouple reading to the reference surface. The maximum variation of the measured wall temperatures of the heater rod and bulk fluid temperatures (k-type thermocouples) was ±1 °C. The bubble diameters could be measured with an accuracy of ±1 *pixel* which comes to about 2.25% for a bubble diameter of about 3 mm. The error in time measurement comes from the speed of the camera, and is of nearly 1 ms.

The heat flux uncertainty was estimated by considering uncertainties of voltage, current, and heated surface area.

$$\frac{\delta q''}{q''} = \sqrt{\left(\frac{\delta V}{V}\right)^2 + \left(\frac{\delta I}{I}\right)^2 + \left(\frac{\delta D}{D}\right)^2 + \left(\frac{\delta L}{L}\right)^2} \tag{4.5}$$

The heat transfer coefficient uncertainty was calculated as

$$\frac{\delta h}{h} = \sqrt{\left(\frac{\delta q''}{q''}\right)^2 + \left(\frac{\delta(\Delta T)}{(\Delta T)}\right)^2} \tag{4.6}$$

The uncertainty of each measured parameter has been given in Table 4. 4.

**Table 4.4** The uncertainties of measured variables

| Variable | Uncertainty value (%) |
|---|---|
| Temperature | $\pm 1.75$ |
| Mass Flux | $\pm 2.5$ |
| Voltage | $\pm 0.5$ |
| Current | $\pm 1.35$ |
| Diameter | $\pm 1.5$ |
| Length | $\pm 1.35$ |
| Bubble Diameter | $\pm 2.25$ |
| Data Signal | $\pm 0.02$ |
| Thermal Conductivity | $\pm 1.5$ |
| Viscosity | $\pm 1.0$ |

The maximum possible error for the parameters involving in analysis have been estimated and summarized in Table 4.5.

**Table 4.5** Uncertainties in estimated parameters

| Variable | Uncertainty value (%) |
|---|---|
| Heat flux ($q''$) | 2.56 |
| Heat transfer coefficient ($h$) | 3.1 |
| Reynolds number ($Re$) | 3.08 |
| Nusselt number ($Nu$) | 3.69 |

## 4.7 Summary

This chapter generated a discussion on experimental setup employed in this research work. It opened up with a description on the instrumentation of the experimental set up and went on to present data analysis and uncertainty analysis. Further, the information regarding high speed camera and image processing have been given in this chapter.